

## Synthesis and characterization of silica mesoporous materials from barley bran for removal of methylene blue

M. Raoui<sup>a</sup>, O. Mohammedi<sup>a</sup>, N. Bouchenafa-Saib<sup>a\*</sup>

<sup>a</sup>. Laboratoire de chimie physique des interfaces des matériaux appliqués à l'environnement, Faculté de Technologie Université Blida 1, B.P. 270 route de Soumaa, Blida 09000, Algérie.

\*Corresponding author: naima\_bouchenafa@yahoo.fr. Tel: +213 555 48 78 04.

### ARTICLE INFO

#### Article History :

Received : 24/02/2020

Accepted : 02/09/2020

#### Key Words:

barley bran;  
sol gel method;  
Adsorption kinetics;  
Isotherm;  
MB dyes;  
silica powder;  
bio-SBA-15;

### ABSTRACT/RESUME

**Abstract:** The recovery and reuse of natural resources can lead to an important economy in the synthesis of materials. In order to prepare meso-structured materials, silica is an essential precursor. This study aims to find a new and less expensive source of silica to replace the one being used currently. It was mainly focused on the synthesis of organized mesoporous silica catalysts (OMS) by the sol-gel process. The bio-SBA-15 was synthesized using Algerian natural resources, such as barley bran and the extracted white powder was characterized by Fourier transform infrared spectroscopy (FTIR). This resulted in the presence of peaks as well as the XRF data proving the presence of silica in the extracted white powder with majority amounts, superior than 98.4%. Therefore, the prepared mesoporous samples were characterized by the different physicochemical methods (x-ray diffraction XRD, scanning electron microscopy SEM, N<sub>2</sub> physisorption, and transmission electron microscope TEM) in order to determine the structural and textural properties of the material. The type IV adsorption isotherm with hysteresis and X-ray diffraction results obtained for bio-SBA-15 show that the mesoporous material exhibited similar results to the material SBA-15 synthesized with the same method with a classic source of silica with a high surface specific area 635 m<sup>2</sup>/g and a pore volume diameter of 0.668 nm. Different parameters were studied to examine the adsorption performance, such as the effect of adsorbent material dosage, initial concentration dye of MB, and pH. Langmuir and Freundlich adsorption models which were recorded to define the equilibrium isotherms. The results show the good efficiency of Methylene Blue adsorption onto bio-SBA-15.



**Schema1.** schematic abstract. A, method was chosen to extract a silica powder from plant biomass and synthesis procedure of silica material. B, synthesis used for mesoporous silica bio-SB-15

## I. Introduction

Important steps have been successfully achieved in the synthesis, characterization, and control of texture and structure parameters of ordered mesoporous silica according to IUPAC (pore size: 2-50 nm). Organized mesoporous silica (OMS), has captured the interest of many researchers. This interest is justified by the physic-chemical properties such as the regular arrangement of channels, adjustable pore size as well as the specific area reaching 1000 m<sup>2</sup>/g. The discovery of the organized mesoporous silica supports has offered a new prospect due to the fact that attaching organic molecules to the non-organic mesostructured shape of the material was made possible.

Mesoporous material is also a promising substance for a lot of applications including separation [1], removal of pharmaceutical pollution [2], controlled drug delivery and catalysis [3,4], electrochemical capacitors [5], anode for lithium-ion batteries [6], as well as being used as an adsorbent of dyes from contaminated waters treatment [7,8].

OMS is usually synthesized according to the cooperative templating mechanism CTM which consists of poly-condensing a non-organic precursor (SiO<sub>4</sub>) around micelles of surfactants in aqueous solution.

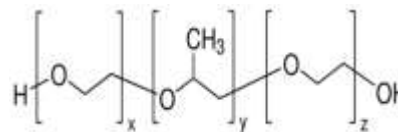
Depending on the surfactant nature used (ionic or non-ionic) and the reaction environment (acid or basic), different material families could be obtained (M41S, SBA-n, HMS, MSU...). In our study, we focused on the SBA-n family (Santa Barbara Amorphous) especially SBA-15, this material was prepared according to the procedure described by Zhao et al [9]. The organized mesoporous silica material (OMS) SBA-15 was synthesized using silica sources and a copolymer that is also known as Pluronic P123, this surfactant is an amphiphilic block copolymer consisting of ethylene oxide and propylene oxide units (EO<sub>20</sub>PO<sub>70</sub>EO<sub>20</sub>) used as a template to have a 2D hexagonal structure (P6mm) with a structure presented in schema 2.

There are various natural resources that allow obtaining silica powder setting apart the sand as a renewable resource a diatomite [10], rice husk [11, 12, 13], the horsetails [14], the fern eagle [15], reed Leaves [5], and a wheat bran [16].

Biomass has a great consideration to extract silica powder [17] for preparing mesoporous materials. Our objective in this study is to use a green process to extract a silica powder from barley bran and prepare ordered mesoporous silica (OMS) materials using the sol-gel methods. The barley bran as a new agricultural waste is a sustainable silica source for amorphous silica.

Almost billions of tons of cereals are produced yearly in the world. The average production of barley in Algeria is 2.5 million of tons. Barley bran is an agricultural waste with a chemical composition

which is similar to many organic fibers, it contains cellulose, lignin, hemicelluloses, and variable amounts of metallic impurities along with silica that is our major component.



Schema 2. Structure of copolymer pluronic p 123.

## II. Materials and methods

### II.1. Pretreatment of the barely bran

The treatment consisted of washing the barely bran with distilled water to remove dust, impurities, and other contaminants, then letting it dry for 48 hours at room temperature (25 ± 1°C). In a three-neck round-bottom flask equipped with a reflux condenser, 50 g of barley bran were attacked first with 15% HCl and then with 35% of H<sub>2</sub>SO<sub>4</sub> at 85°C for 2 hours. The obtained mixture was filtered and washed several times with distilled water. The solid neutralization control was done using the pH meter measurement of washing water until the constant pH. After the neutralization, the solid dried at 80°C for 12 hours. Finally, the samples were calcined at 600°C with a ramp rate of 5°C / min for 24 hours.

### II. 2. Preparation of Mesoporous Silica Material

#### II. 2. 1. Preparation of sodium silicate solution

Sodium silicate was prepared by reflux. The solid obtained was mixed with 2M NaOH solution and heated at 85°C for 4 hours under fast and constant stirring. After that, the solution was filtered and stored until usage.

#### II. 2. 2. Synthesis of SBA-15

The ordered mesoporous silica matrix SBA-15 was prepared in hydrothermal conditions [18]. 3.5 g of P123 copolymer (Mw 45800, Aldrich) was dissolved in 112 ml of bi-distilled water and 16.5 ml of concentrated HCl (37% in weight, Fluka). The mixture was then heated up to 40°C and maintained under strong and continuous stirring for 3 hours. Next, 7.43 g of tetraethylorthosilicate TEOS (98%, Aldrich) was added to the solution and the mixture was stirred at a temperature of 40°C for 24 hours then put in the oven at 100°C. The resulting mixture was then transferred to an oven and heated at 90°C for 24 hours.

Finally, the mixture was recovered by centrifugation at 6000 rpm/min and washed with distilled water as well as dried at 70°C for 48 hours. The surfactant was removed by calcination at 500°C for 4 hours under air.

### II. 2. 3. Synthesis of bio-SBA-15

The bio-SBA-15 material which is the synthesized mesoporous silica material with a new silica source, was prepared in the following way: 2, 9 g of copolymer P123 were dissolved in 115 ml of bi-distilled water and 5, 8 ml of pure HCl (37% in weight, Fluka). The mixture has gone through a heating treatment at 37°C under 600 tour/min of stirring for 3 hours. A quantity of 26 ml of sodium silicate solution was added dropwise to the mixture, after that another stirring at 37°C was done for 24 hours. It was then heated at 90°C for 48 hours. The resulting mixture was filtered and washed several times using distilled water then dried at 90°C. Finally, the powder was calcined under air at 550°C for 6 hours.

### II. 3. Material characterization

#### II. 3. 1. The Characterization of Silica Powder

The quantitative chemical analysis of barely bran before and after treatment were performed by X-ray fluorescence (XRF PANanalytical epsilon 3-XL), the characterization of extract silica powder (white SiO<sub>2</sub> powder) obtained after chemical treatment was performed by Fourier transform infrared spectroscopy (BRUKER OPUS 7518), and the microstructural images and morphology of the sample were obtained by scanning electron microscopy (Gemini SEM 300).

#### II. 3. 2. The Characterization of Mesoporous Silica Materials

The mesoporous materials were characterized through X-ray diffraction using a Bruker AXS D8 Advance. The textural properties data, such as specific surface area and pore size distribution of the mesoporous materials were recorded using BET and BJH methods at -196°C, using N<sub>2</sub> physisorption analyzer (Micromeritics ASAP 2420). The pore structure and morphology of silica materials were observed with Transmission Electron Microscopy (JEOL JEM-2001).

### III. Adsorption experiments

The adsorption kinetics experiments were carried out in batch and in glass bottles of 250 ml using a laboratory shaker (Edmund Bühler GmbH) at 250 rpm, and at temperature (25 ± 1° C). Each bottle contains a constant volume of 20 ml that was performed at concentrations of 20 mg/L and an adsorbent material dose of 0, 04 g to calculate the effect of contact time.

The mixtures were recovered, and the obtained samples were analyzed using the UV-VIS spectrophotometer (UV 1800 Shimadzu spectrophotometer) with a wavelength λ<sub>max</sub>= 639

nm of methylene blue dye. The different properties and structure of methyl blue are shown in table 1. Other parameters and conditions such as the effect of adsorbent material dosage, initial concentration of MB dye, and pH were recorded. The removal quantities and adsorption amount of MB were calculated by using the following equations, respectively:

$$\% = [(C_0 - C) / C_0] * 100 \quad (1)$$

$$q_e = [(C_0 - C_e) * V / W] \quad (2)$$

C<sub>0</sub> represents the initial concentration, C<sub>e</sub> is the equilibrium concentration, and V and W are the volume of the solution and the mass of the adsorbent respectively.

### IV. Results and discussion

#### IV. 1. Characterizations of silica powder and mesoporous silica materials:

XRF results obtained from the barley bran before and after chemical treatment were presented in the table 2. The chemical attack leads to the elimination of the different elements which were present in the barley bran as explained previously. These phenomena were shown earlier by the decrease of their composition and enrichment of silica in the treated material. Furthermore, the silica is not soluble in the acid and is still maintained in the material.

Fourier transform infrared spectra of silica powder extracted from barely bran showed in fig.1, the major peaks of SiO<sub>2</sub> groups appearing at 1123, 788, 476 cm<sup>-1</sup> were produced to the extending and deformation vibrations [19], and the band at 1645 cm<sup>-1</sup> is about Si-OH [20,21]. These confirmed a pure silica powder because there were no other adsorption peaks.

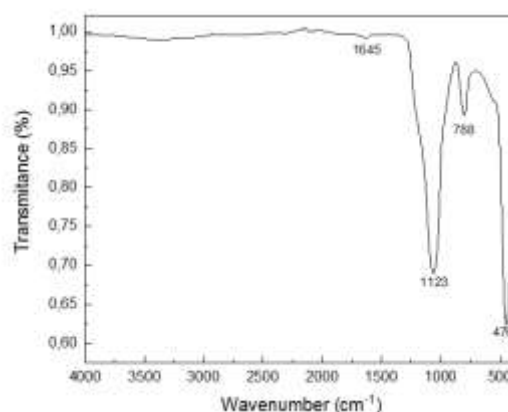
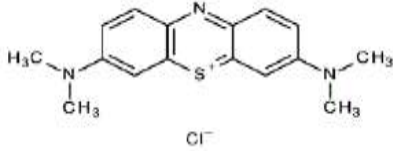
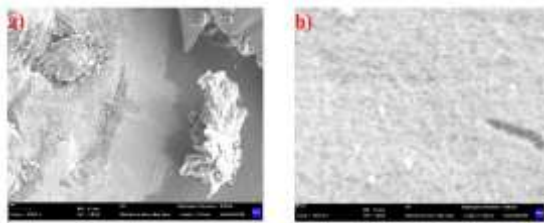


Figure 1. FT-IR spectra of extracted silica powder

**Table 1.** Different properties of the methylene blue.

Name	wave length (nm)	Type	Pka	Solubility in water	molar structure
methylene blue (methylthioninium chloride)	664	cationic dye	3.8	4.36 g/100 ml (25 °C)	

The spectra of microstructure of the silica powder are shown in fig.2. These were examined and characterized the morphology of the sample [22,23]. The results were obtained after the chemical treatment and the decomposition of organic matters during the calcination of barley bran. The analysis of white powder exposed in fig. 3, using energy dispersive spectroscopy (EDS) revealed the existence and the percentage of Si and O elements. Supplementary verification of an efficient extraction of SiO<sub>2</sub> from natural source [19].



**Figure 2.** SEM image of silica powder a) at 30 μm, b) at 60 μm.

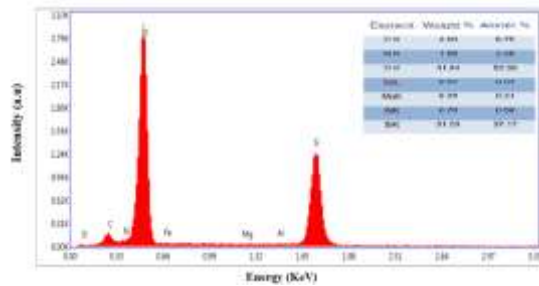


**Figure 3.** The EDS spectrum of Si and O elements of silica powder.

**IV. 2. Characterizations of mesoporous silica**

A small angle Powder X-ray diffraction (XRD) pattern of mesoporous SBA-15 and bio-SBA-15 depicted in the figure 4 were used. Clearly, three broad diffraction peaks (100), (110), and (200) were identified. These explaining that the material has a mesoporous hexagonal structure (space group p6mm) [24].

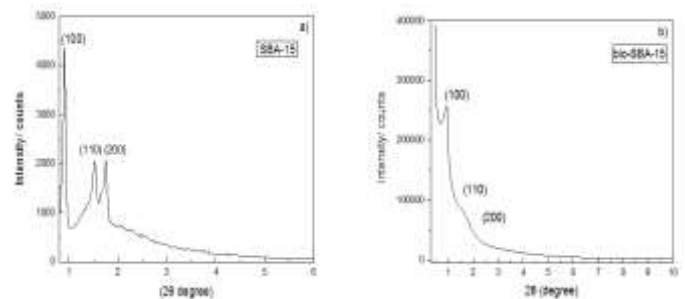


**Figure 4.** XRD pattern of the a) SBA-15 and b) bio-SBA-15 mesoporous materials.

The isotherm N<sub>2</sub> adsorption–desorption of the synthesized materials elucidated in fig.5. It is visibly seen that the isotherms have exhibited a type IV curve with a hysteresis confirming the formation of a mesoporous structure. The specific surface area of the samples, according to the BET equation, was 635 m<sup>2</sup>/g and 921 m<sup>2</sup>/g for bio-SBA-15 and SBA-15 respectively. Moreover, the BJH pore volume diameter is approximately 0.668 nm of bio-SBA15 and 0. 894 nm of SBA-15.

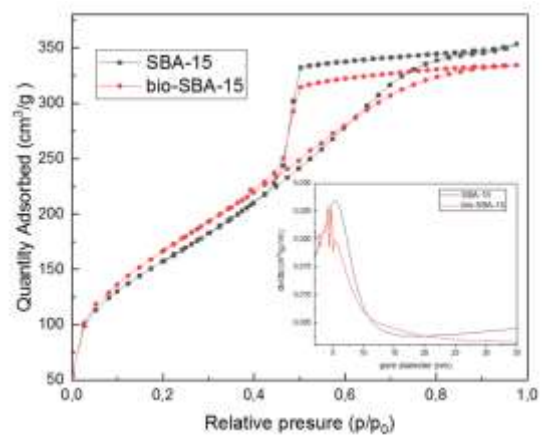


**Figure 5.** The N<sub>2</sub> adsorption–desorption isotherms of SBA-15 and bio-SBA-15.

Table 2. Chemical compositions of the barley bran.

Component (wt.)	Al <sub>2</sub> O <sub>3</sub>	SiO <sub>2</sub>	P <sub>2</sub> O <sub>5</sub>	SO <sub>3</sub>	K <sub>2</sub> O	CaO	TiO <sub>2</sub>	MnO	Fe <sub>2</sub> O <sub>3</sub>
(%) Before treatment	0,1678	47,5131	9,2770	5,1170	20,7971	21,3470	0,14480	0,3706	4,1500
(%) After treatment	0,4230	98,4270	0,5748	0,0164	0,0754	0,2599	0,0454	0,0025	0,9426

The structure of materials is also clear in the TEM images, as shown in Figure 6, the bio-SBA-15 exhibits an ordered hexagonal structure with parallel channels having comparable morphology obtained from SBA-15 synthesized with classical silica source.

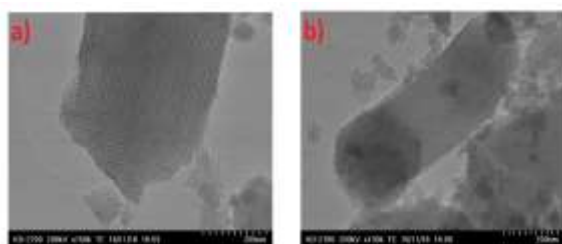


Figure 6. TEM images of mesoporous materials: a) SBA-15 and, b) bio-SBA-15.

## V. Adsorption studies

### V.1. Effect of contact time

This study was conducted to determine the required contact time to achieve the adsorption equilibrium. The reaction time is one of the most important factors that influence the adsorption process of dye [25]. As shown in fig.7, the efficiency adsorption of dye by bio-SBA-15 adsorbent was increased with the increasing time. Thus, more than 99% of the dye can be quickly removed, and adsorption equilibrium can be achieved within 10 min.

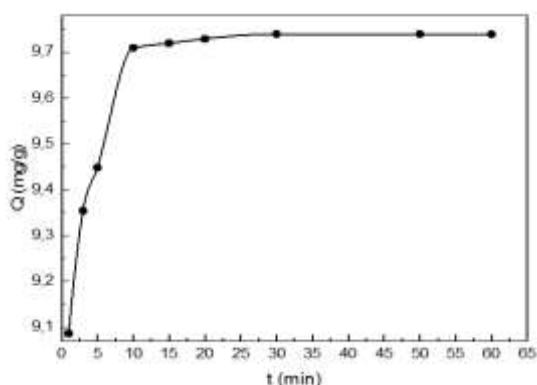


Figure 7. The effect of contact time of bio-SBA-15 adsorbent.

### V. 2. Effect of pH

In the adsorption process, the pH effect is a very important parameter and its behavior depends strongly on  $pH_{PZC}$  value which equals 6 for bio-SBA. The pH was adjusted by the addition of HCl or NaOH. The results were illustrated in the fig. 8. It was observed that the amount of adsorbed methylene blue by bio-SBA-15 remained constant at the pH range from 2 to 6, in this field of pH, the surface of biomaterial is positively charged leading to repulsion between the surface material and the methylene blue cations. At range from 6 to 10 ( $pH \geq pH_{pzc}$ ), we have an attractive interaction between the surface of bio-SBA-15 which became negatively charged and MB aromatics cations, this attraction results in an increase in adsorbed quantity with an optimum pH of 10 for MB adsorption onto bio-SBA material. Finally, at pH values superior than 10, a decrease of adsorption in a fast way is to be noticed, therefore, the great basicity does not promote the adsorption of the MB dye. This decrease in adsorption was explained by the high abundance of OH<sup>-</sup> ions in the solution created by the addition of NaOH, these provoke a competitive environment with anionic ions for adsorption sites [26].

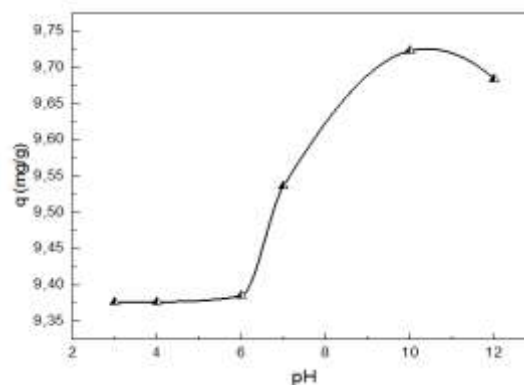
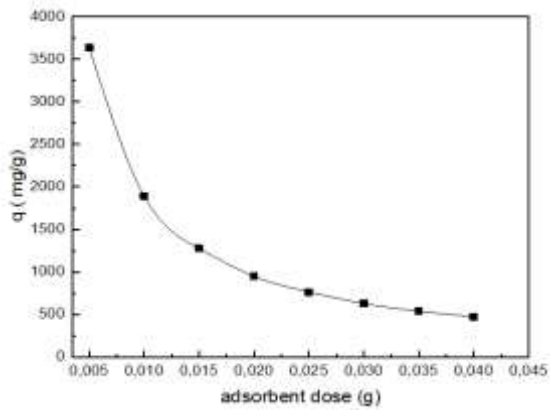


Figure 8. The effect of pH on the adsorption of MB dye by bio-SBA-15 adsorbent.

**V. 3. Effect of adsorbent dose**

A series of experiments was made to define the optimum dose of adsorbent needed to remove the MB dye. The effect of the adsorbent mass on the adsorption of methylene blue was studied by varying the dose of mesoporous adsorbent from  $5 \times 10^{-3}$  to  $4 \times 10^{-2}$  g. The methylene blue dye concentration was tested at the same previous conditions of adsorption study. The result elucidates in the fig.9, which shows a decrease of the amount in adsorbed dye with an increase in the adsorbent dose. The removal efficiency of dye increases quickly with the increasing of the adsorbent dose, this is due to the high specific surface area owing to the increase in the mass of the adsorbent so it has more adsorption sites [27,28].



**Figure 9.** Influence of bio-SBA-15 dose adsorbent on the amount of adsorbed dye.

**V. 4. Adsorption kinetics**

To study the adsorption kinetic characteristics of the silica material, the kinetic models of pseudo-first-order and pseudo-second-order were utilized, their linear forms are given by equations (3) and (4) respectively.

**V. 4. .1 Pseudo first order model**

The pseudo-first-order equation is given as:

$$\log(q_e - qt) = \log q_e - \frac{k_1}{2.303} t \quad (3)$$

While  $q_e$  and  $q_t$  ( $\text{mg. g}^{-1}$ ) represent the amount of dye adsorbed at equilibrium and time  $t$  (min) respectively,  $k_1$  represents the pseudo-first-order rate coefficient.

As depicted in Fig. 10, (a) and Table 3, the data record does not conform with the pseudo-first-order equation with  $R^2$  value of 0.981.

**V. 4. 2. Pseudo second order model**

The pseudo-second-order equation is given as:

$$\frac{1}{q_t} = \frac{1}{k_2 q_e^2} + \frac{1}{q_e} t \quad (4)$$

$k_2$  represents the rate coefficient of the pseudo-second-order ( $\text{g.mg}^{-1}$ ).

As shown in Fig. 10, (b), it was concluded that the pseudo second order is the predominant model and confirms the process of adsorption with  $R^2$  value of 0.9999.

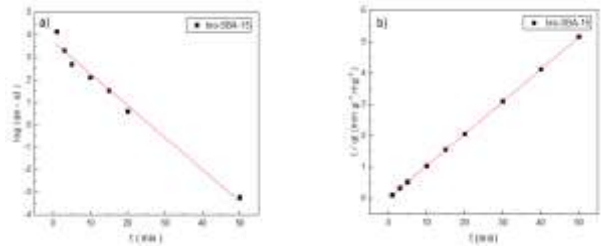


**Figure 10.** (a) pseudo-first-order adsorption kinetics plot, (b) pseudo-second-order adsorption kinetics plot.

**V. 5. Equilibrium adsorption models**

The generally utilized adsorption isotherm models namely Langmuir and Freundlich models were applied in this study. Langmuir and Freundlich isotherms parameters can be obtained from their linear forms they are habitually described by (5) and (6) equations respectively:

$$\frac{C_e}{q_e} = \frac{1}{k_1} + a \frac{C_e}{k_1} \quad (5)$$

While  $q_e$  and  $C_e$  represent the amount of adsorbed ( $\text{mg. g}^{-1}$ ) and the equilibrium concentration of MB dye solution ( $\text{mg. l}^{-1}$ ), respectively,  $K_1$  ( $\text{l.mg}^{-1}$ ) represents the Langmuir constant.

The Freundlich isotherm which is an empirical model is not only by limited by the monolayer adsorption, it is expressed as:

$$\ln q_e = \ln k_F + \frac{1}{n} \ln C_e \quad (6)$$

Table 3. Kinetic parameters for MB dye onto the bio-SBA-15 adsorbent.

Pseudo first order model			Pseudo second order model		
q <sub>cal</sub> (mg/g)	K <sub>1</sub> (min <sup>-1</sup> )	R <sup>2</sup>	q <sub>cal</sub> (mg/g)	K <sub>2</sub> (g/mg)	R <sup>2</sup>
4897.78	0.327	0.981	9.80	0.645	0.9999

n = 0.24 represents the intensity factor while K<sub>f</sub> = 7.25 (L/mg) represents the constant of Freundlich, these can be taken from the plot as the slope and intercept respectively.

As presented in fig. 11, The Freundlich model seems to be more well described than the Langmuir one due to the High value of R<sup>2</sup>. It is also noted that the removal of BM occurs on multilayer adsorption [29,30].

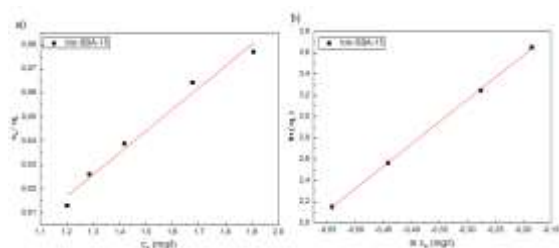


Figure 11. (a) Langmuir isotherm model, (b) Freundlich isotherm model.

## VI. Conclusion

This study has come to the conclusion that barley bran is a renewable silica source with low-cost. For the preparation of silica mesoporous materials, it is best to use a simple chemical treatment to extract the silica powder and prepare bio-SBA-15 materials with the same textural and structural properties as the classic materials. Moreover, the surface area of the bio-SBA-15 sample synthesized was found to be 635 m<sup>2</sup>/g. Furthermore, the pore volume diameter of the bio-SBA-15 material was 0.668 nm. X-ray diffraction (XRD), TEM analysis, and BET results of bio-mesoporous silica proved their nearness of structural and textural properties to those obtained from conventional silica resources.

The adsorption tests confirmed that the bio-mesoporous silica material (bio-SBA-15) synthesized from barley bran as a silica resource had good adsorption capacity for MB in aqueous solutions. Kinetic and isotherm model analysis disclosed that the experimental data fit well the pseudo-second-order model and Freundlich isotherm, respectively.

## Acknowledgements

The authors thank the direction of scientific research and technological development (DGRSDT) for funding the laboratory CPIMAT that led to this publication. The authors thank also Plasma & Applications team of CDTA for physico-chemical characterization.

## VII. References

1. Corma, A. From Microporous to Mesoporous Molecular Sieve Materials and Their Use in Catalysis. *Chemical Reviews*. (2002) 97, 2373–2420.
2. Chauhan, M.; Saini, V.; K. & Suthar, S. Removal of pharmaceuticals and personal care products (PPCPs) from water by adsorption on aluminum pillared clay. *Journal of Porous Materials*. (2019) 019-00817-8.
3. Yang, Y.; Zhuang, Y.; He, Y.; Bai, B.; Wang, X. Fine tuning of the dimensionality of zinc silicate nanostructures and their application as highly efficient adsorbents for toxic metal ions. *Nano Research*. (2010) 3, 581–593.
4. Ganesh Kumar, C.; Poornachandra, Y.; Pombala, S. *Therapeutic nanomaterials: from a drug delivery perspective. Nanostructures for Drug Delivery* (2017) 6.00001-4.
5. Zhao, J.; Zhang, Y.; Wang, T.; Li, P.; Wei, C. Reed Leaves as a Sustainable Silica Source for 3D Mesoporous Nickel (Cobalt) Silicate Architectures Assembled into Ultrathin Nanoflakes for High-Performance Supercapacitors. *advanced material interface* (2015) 1–10.
6. Xing, A.; Tian, S.; Tang, H.; Losic, D.; Bao, Z. Mesoporous silicon engineered by the reduction of biosilica from rice husk as a high-performance anode for lithium-ion batteries. *RSC Advanced*. (2013) 3, 10145–10149.
7. Nicola, R.; Costișor, O.; Gabriel, S.; muntean, S.; Nistor, M.; Putz, A.; Ianăși, C.; Lazău, R.; Almásy, L.; Săcărescu, L.; Mesoporous magnetic nanocomposites: a promising adsorbent for the removal of dyes from aqueous solutions. *Journal of Porous Materials*. (2019).10934-019-00821.
8. Thien, N.; Shiao-Shing, C.; Nguyen Cong, N.; Hau Thi, N.; Hsiao Hsin, T.; Tang, C. Adsorption of Methyl Blue on Mesoporous Materials Using Rice Husk Ash as Silica Source. *Journal of nanoscience and nanotechnology*. 4108–4114 (2016).2016.10704
9. Zhao, D.; Huo, Q.; Feng, J.; Chmelka, B. F.; Stucky, G. D. Nonionic triblock and star diblock copolymer and oligomeric surfactant syntheses of highly ordered, hydrothermally stable, mesoporous silica structures.

- Journal of American Chemistry Society.* (1998) 120, 6024–6036.
10. Process, I. J. M.; Osman, Ş.; Gören, R.; Özgür, C. Purification of diatomite powder by acid leaching for use in fabrication of porous ceramics. *International Journal of Mineral Processing.* (2009) 93, 6–10.
  11. Morawala, D.; Dalai, A.; Maheria, K. Rice husk mediated synthesis of meso-ZSM-5 and its application in the synthesis of n-butyl levulinate. *Journal Porous Materials.* (2019) 26, 677–686.
  12. Bhagiyalakshmi, M.; Lee, J. Y.; Jang, H. T. International Journal of Greenhouse Gas Control Synthesis of mesoporous magnesium oxide: Its application to CO<sub>2</sub> chemisorption. *International Journal of Greenhouse Gas Control* (2010) 4, 51–56.
  13. Nur, H.; Guan, L. C.; Endud, S.; Hamdan, H. Quantitative measurement of a mixture of mesophases cubic MCM-48 and hexagonal MCM-41 by <sup>13</sup>C CP/MAS NMR. *Material Letter.* (2004) 58, 1971–1974.
  14. Law, C.; Exley, C. New insight into silica deposition in horsetail (*Equisetum arvense*). *BMC Plant Biology.* (2011)11, 112.
  15. Laroche, J.; Guervin, C.; Lecoq, C.; Robert, D. Activités pétrogénétiques chez *Equisetum arvense* L. (ptéridophytes). *Bulletin de la Société Botanique de France.* (1992). 139, 47–55
  16. Raoui, M.; Saib, Bouchenafa. N.; Mohammedi, O. Etude comparative d'un support silicique synthétisé à partir des sources naturelles. *ipco Academy* (2017) 4–7.
  17. Soltani, N.; Bahrami, A.; Pech-Canul, M. I.; González, L. A. Review on the physicochemical treatments of rice husk for production of advanced materials. *Chemical Engineering Journal.* (2015) 264, 899–935.
  18. Benamor, T.; Vidal, L.; Lebeau, B.; Marichal, C. Influence of synthesis parameters on the physicochemical characteristics of SBA-15 type ordered mesoporous silica. *Microporous Mesoporous Materials.* (2012)153, 100–114.
  19. Zhang, S.; Gao, H.; Li, J.; Huang, Y.; Alsadic, A.; Tasawar, H.; Xu, X.; Wang, W. Rice husks as a Sustainable Silica Source for hierarchical flower-like metal silicate architectures assembled into ultrathin nanosheets for adsorption and catalysis. *Journal of Hazardous Materials.* (2016).2016.09.004.
  20. Zhang, S.; Xu, W.; Zeng, M.; Lie, J.; Xub, J.; Wang, X. Superior adsorption capacity of hierarchical iron oxide@magnesium silicate magnetic nanorods for fast removal of organic pollutants from aqueous solution. *Journal. Materials. Chemistry. A* (2013).1, 11691–11697.
  21. Takahashi, R.; Sato, S.; Sodesawa, T.; Kawakita, M.; Ogura, K. High surface-area silica with controlled pore size prepared from nanocomposite of silica and citric acid. *Journal of Physical Chemistry B* (2000). 104, 12184–12191.
  22. Abro, D. M. K.; Dable, P. J. M. R.; Amstutz, V., Kwa-Koffi, E. K. & Girault, H. Forced Electrocodeposition of Silica Particles into Nickel Matrix by Horizontal Impinging Jet Cell. *Journal of Materials Science and Chemical Engineering.* (2017) 05, 51–63.
  23. Potapov, V.; Serdan, A.; Gorev, D.; Zubaha, S.; Shunina, E. Colloid silica in hydrothermal heat carrier: Characteristics, technology of extraction, industrial applications. *IOP Conference Series.* (2019) 249, 1254–189.
  24. Kruk, M.; Jaroniec, M.; Ryoo, R.; Kim, J. M. Characterization of High-Quality MCM-48 and SBA-1 Mesoporous Silicas. *Chemistry of Materials* (1999) 2568–2572.
  25. Pei, Y.; Jiang, Z.; Yuan, L. nanocomposites with ultrahigh adsorption performance and excellent recycling. *Colloids and Surfaces A: Physicochemical and Engineering Aspects* (2019) 123816.
  26. Hussain, I.; Li, Y.; Qi, J.; Li, J.; Wang, L. Nitrogen-enriched carbon sheet for Methyl blue dye adsorption. *J. Environ. Manage.* (2018) 215, 123–131
  27. Yu, Z.; Zhai, S.; Guo, H.; Ming, T.; Song, Y.; Zhang, F.; Ma, H. Removal of methylene blue over low-cost mesoporous silica nanoparticles prepared with naturally occurring diatomite. *Journal of Sol-Gel Science and Technology.* (2018) 88, 541–550.
  28. Fungaro, D. A.; Bruno, M.; Grosche, L. C. Adsorption and kinetic studies of methylene blue on zeolite synthesized from fly ash. *Desalination and Water Treatment.* (2009)2, 231–239.
  29. Lin, L.; Zhaia, S.; Xiao, Z.; Song, Y.; Ana, Q.; Sonc, X. Dye adsorption of mesoporous activated carbons produced from NaOH-pretreated rice husks. *Bioresour. Technology.* (2013) 136, 437–443.
  30. Erfani, M.; Javanbakht, V. Methylene Blue removal from aqueous solution by a biocomposite synthesized from sodium alginate and wastes of oil extraction from almond peanut. *International Journal of Biological Macromolecules.* (2018)114, 244–255.

**Please cite this Article as:**

Raoui M., Mohammedi O., Bouchenafa-Saib N., Synthesis and characterization of silica mesoporous materials from barley bran for removal of methylene blue, ***Algerian J. Env. Sc. Technology, 7:4 (2021) 2107-2114***